

# How to reduce Covid-19 transmission in a small meeting room using a Mixed Ceiling Ventilation system.

Wenyan Cai\*<sup>1</sup>, R.M.J. Bokel\*<sup>1</sup>, Peter van den Engel<sup>1</sup>

*1 Delft University of Technology  
Julianalaan 134  
2628 BL Delft, The Netherlands*

*\*Corresponding authors: R.M.J.Bokel@tudelft.nl*

## ABSTRACT

Building system engineering can help decrease the risk of being infected by the aerosol which contains virus-laden droplet nuclei. Many techniques can help decrease the concentrations of particles. This paper focuses on the economic renovation of the existing ventilation system of a public commercial space, a small meeting room in Kuijpers, Leiden, to decrease airborne transmission of respiratory infectious diseases. Simulations and measurements show the effect of different mixed ceiling (VRF) ventilation configurations on Covid-19 transmission with and without filters in Dutch offices.

## KEYWORDS

Local air recirculation, mixing ventilation, office hygiene ventilation, airborne transmission, respiratory diseases control, filters

## 1 INTRODUCTION

The coronavirus pandemic is caused by the newly discovered coronavirus SARS-CoV-2. All societies are desperate for a series of solutions to improve the public safety through epidemic prevention. From the state to social groups to individuals, various levels of society have taken different epidemic prevention measures. The Dutch government has introduced restrictions on the size of groups, social distance limits and the closure of non-essential business premises. COVID-19 changes everyone's daily life from all aspects but everyone tries to minimize the impact of the epidemic on people's daily life.

Airborne transmission is one of the three commonly accepted transmission modes for person-to-person respiratory infectious diseases, like COVID-19. The other two valid transmission routes are direct contact with virus-laden surfaces and exposure to the respiratory droplets from effected people (Morawska et al., 2020). These two transmission methods can be cut off by personal hygiene protection, like washing hands frequently, keeping a safe social distance and wearing masks. But for airborne transmission, it is hard to predict the airflow or make personal protection. The most influential engineering method for the general public to decrease the infection risks is ventilation (Morawska et al., 2020).

After the COVID-19 crisis the role of offices is changing. Special tutoring, group discussions and activities need direct feedback to ensure necessary collaboration. Thus, small-scale meeting rooms are quite needy in COVID-19 crisis and play a future role in offices.

The idea is to find a ventilation strategy to control or at least reduce the risk of respiratory infections via airborne transmission and meet the requirements of indoor comfort and reasonable economic costs in a typical meeting room. A widely applied ventilation system in Dutch offices and elsewhere in the world is a fan-coil air-recirculation indoor end unit with mixing ventilation. In this research the meeting room in the Kuijpers office, Leiden was used as a case study.

## 2 THEORY

### 2.1 Particle sizes

The COVID-19 virus nuclei has sizes from 0.005  $\mu\text{m}$  to 0.3  $\mu\text{m}$ . Virus nuclei can be minimally attached to particles as large as they are. Particles of various sizes are produced during breathing, talking, coughing and sneezing. Morawksa (2009) measured particle sizes between 0.3  $\mu\text{m}$  and 20  $\mu\text{m}$ . Breathing produced mainly particle sizes between 0.3 and 1.5  $\mu\text{m}$ . Talking (counting and producing an “aah” sound) increased the amount of particles in the range between 0.3  $\mu\text{m}$  and 1.5  $\mu\text{m}$  and added a significant amount of particles sizes between 1.5 and 5.0  $\mu\text{m}$ . Large droplets, though, were indicated to be mainly generated by sneezing and coughing, at a relatively low density (Ding et al., 2022). However, the relationship between the viral load and different aerosol sizes is still unknown, which makes the estimation of infectivity principally hard. This paper assumes that all particles contain a viral load.

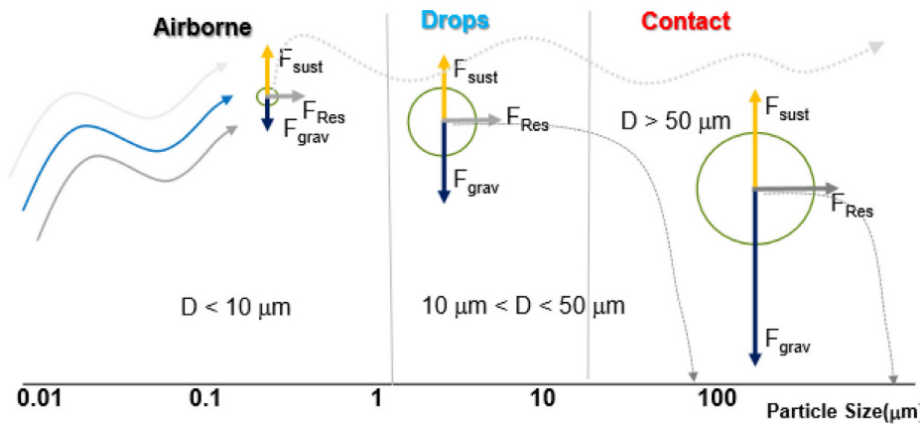


Figure 1: Trajectories of particles with various sizes (Lipinski et al., 2020)

Figure 1 shows the trajectories for particles of various sizes ranging from 0.01  $\mu\text{m}$  to 100  $\mu\text{m}$ . Larger particles have the tendency to settle. Smaller particles are more likely to be airborne (Lipinski et al., 2020). Sadly the WHO at first considered coughing and sneezing as the main source of transmission and assumed that particles larger than 5 $\mu\text{m}$  were not airborne, see (Randall et al, 2021), neglecting the effect of aerosol transmission. In reality the airborne particle movement is expansive. The virus nuclei-laid particle of about 0.01 – 0.5  $\mu\text{m}$  is the airborne particle size discussed in this paper.

### 2.2 Infection risk (Wells-Riley model)

There is no direct mathematical method to connect the indoor pathology with detailed ventilation engineering. The Wells-Riley Model is the most ideal mathematical tool to illustrate the infection risk of a space in general. The precondition for Wells-Riley model is that all the cases meet the well-mixing ventilation pattern. Wells proposed a hypothetical infectious dose unit: the quantum of infection. A quantum is defined as the number of infectious airborne particles required to infect a person and may consist of one or more airborne particles. These particles are assumed to be randomly distributed throughout the air of confined spaces. Riley considered the intake dose of airborne pathogens in terms of the number of quanta to evaluate the probability of escaping the infection as a modification of the Reed-Frost equation. Together with the Poisson probability distribution describing the randomly distributed discrete infectious particles in the air, the Wells–Riley equation was derived to be (Sze To et al, 2010):

$$PI = \frac{C}{S} = 1 - e^{-\left(\frac{Iqp t}{Q}\right)} \quad (1)$$

where PI is the probability of infection, C is the number of infection cases, S is the number of susceptible, I is the number of infectors, p is the pulmonary ventilation rate of a person, q is the quanta generation rate, t is the exposure time interval, and Q is the room ventilation rate with

clean air. The minimum breathing volume is  $0.5\text{m}^3/\text{h}$ , which is the minimum volume of respiratory modes for oral breathing when resting, see Buonanno et al., 2020. The quanta generation rate,  $q$ , cannot be directly obtained, but estimated epidemiologically from an outbreak case where the attack rate of the disease during the outbreak is substituted into PI. If the exposure time and ventilation rate are known, the quanta generation rate of the disease can be calculated from the reproductive number.  $q$  is chosen to be **25 quanta/h** based on a reproductive number of 2.0-2.5 (Dai & Zhao, 2020). However, with the omicron- or delta-virus a higher  $q$ -value like 50 may be a more appropriate value for meeting rooms.

The practical ventilation strategy to control the airborne transmission of corona virus will be based on an acceptable risk level. The WHO (World Health Organisation) guidelines for carcinogens is  $10^{-5}$  for a death rate of 8-90% in the UK (Nuffield website), giving a death risk of 90% times  $10^{-5}$  is a  $10^{-4}$  risk of dying from cancer. With a 1.4 % mortality rate of COVID-19 in the Netherlands (Coronavirus Death Rate website) this research chooses a similar COVID-19 risk as the cancer risk of  $10^{-4}$ . This then amounts to a **1% infection risk**, PI, at a mortality rate of 1.4 % ( $1.0\% \times 1.4\% = 1.4 \cdot 10^{-4}$ ).

### 2.3 Clean Room techniques

Building system engineering can help decrease the risk of being infected by the aerosol which containing the virus-laden droplet nuclei. Many techniques in building system can help decrease the concentrations of particles. The six currently practical building engineering technologies are: ventilation, mechanical air filters, UV-lights, bio-polar ionization generators, ozone generating air cleaners and electrostatic precipitator (EPS) (Nafezarefi and Joosten, 2020).

Air clean technology is a new technology, starting from mid-1950s. HEPA filter air clean technology is the most basic and the most necessary means for air clean technology. Other clean room design details, including the position of supply and exhaust openings, dilution efficiency, air quality monitors and air quality smart control are also important in high-hygiene ventilation design. The clean room ventilation, standing for the highest cleanness level in the built environments, will inspire ventilation strategy design for epidemic prevention in a shared space.

### 2.4 Ventilation Design/ Air distribution patterns

Computational Fluid dynamics and measurements are techniques to investigate the ventilation design and the air distribution pattern. The ventilation efficiency is evaluated by air change rate and pollutant removal efficiency based on REHVA Ventilation Effectiveness Guidebook (Mundt et al, 2004):

The air change efficiency,  $\varepsilon^a$ , is defined as:

$$\varepsilon^a = \frac{\tau_n}{2\langle\bar{\tau}\rangle} \cdot 100 \quad (2)$$

with  $\tau_n$  the nominal time constant ( $\tau_n=V/q_v$ ) with  $V$  the room volume and  $q_v$  the ventilation flow rate and  $\langle\bar{\tau}\rangle$  room mean age of air. The general pollutant removal efficiency,  $\varepsilon^c$ :

$$\varepsilon^c = \frac{c_e}{\langle c \rangle} \cdot 100 \quad (3)$$

with  $c_e$  the steady state concentration of the contaminant in the exhaust air and the steady state mean concentration of the room  $\langle c \rangle$ .

The calculation of the infection risk at the breathing height is based on the comparison ratio between the average  $\text{CO}_2$ -concentration at the breathing height in this case,  $c\text{CO}_2(x)$ , and that in the standard case,  $c\text{CO}_2(0)$ . Thus the local infection risk at position  $x$ ,  $PI(x)$ , is:

$$PI(x) = \frac{c\text{CO}_2(x)}{c\text{CO}_2(0)} PI(0) \quad (4)$$

### 3 METHOD

#### 3.1 Description of the room

The test room chosen for the research has a size of  $4.52 \times 5.60 \times 2.80 = 71 \text{ m}^3$ , which is a small meeting room for 6-8 people before corona time. The room is a typical shared space for group work. There is one exhaust opening and one indoor unit with a separated control panel in that space, see figure 2. The exhaust opening is a  $0.6\text{m} \times 0.6\text{m}$  perforated aluminium panel. The only possible way for passive ventilation is an inward-opening bottom-hung window which is closed all the time. The meeting room of Kuijpers Leiden is located on the 5<sup>th</sup> floor of a joint office building for lease in Leiden.

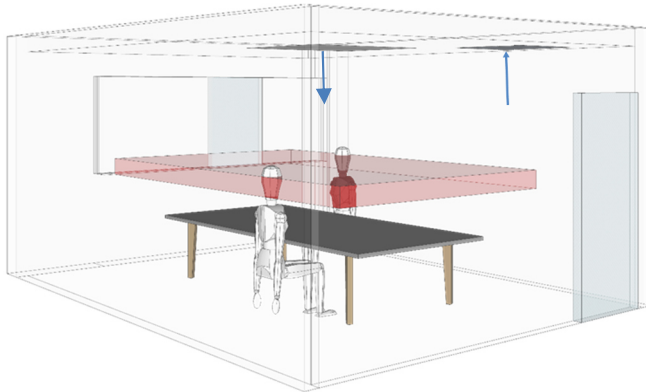


Figure 2: the perspective of the meeting room in Kuijpers, Leiden, as the typical medium-scale environment

#### 3.2 Indoor unit

The indoor unit is a PLFY-P20VLMD-E by Mitsubishi. The mechanism of the indoor unit is shown in figure 3: the recirculated air first goes through the filter for coarse particles, and mixes up with the prime air before fan coil. By the air pressure offered by the fan coil, the mixed air will be heated or cooled by the cross-fin heat exchanger in the unit as the secondary procedure. Then it will be transported to the supply opening and supplied to the space at an angle of  $15^\circ$ .

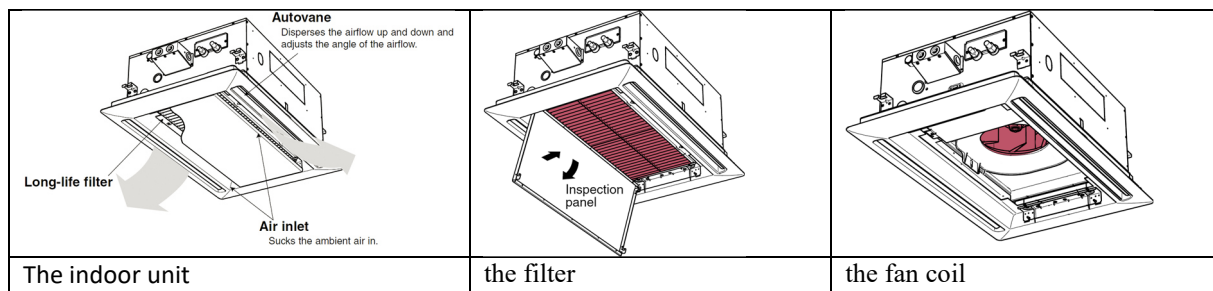


Figure 3: The indoor ventilation unit. The grey arrows show the supplied air. The air inlet is in fact the return opening of recirculated air. The exhaust of the fresh supplied air is on some distance of the fan-coil, see the two grey surfaces at the ceiling of figure 2.

The two supply openings are  $800 \text{ mm} \times 50 \text{ mm}$  with a vane in each to adjust the air flow direction at the angle  $10^\circ - 20^\circ$ , mostly at  $15^\circ$ . The control system is temperature-based with a reaction domain of lower than  $20^\circ \text{C}$  and higher than  $26^\circ \text{C}$ . The filter applied in this indoor unit is a long-life filter made by PP Honeycomb fabric (washable). There are 4 levels of fan speed on the control panel with a maximum of  $9.5 \text{ m}^3/\text{min}$  ( $570 \text{ m}^3/\text{h}$ ).

#### 3.3 Measurements

$\text{CO}_2$ -concentrations and particle counts are measured in the meeting room. The  $\text{CO}_2$ -sensor is a HOBO  $\text{CO}_2$  logger with a measurement range of 0-5000 ppm with an accuracy of 50 ppm or 5% at  $25^\circ \text{C}$ . The particle counter is a MET ONE 3400 series particle counter and measures particle sizes in the range of  $0.3\text{-}10 \mu\text{m}$  with a maximum particle count of 9,999,999. The

accuracy of the particle counter is 5 % at 14,126,000 particles per  $\text{m}^3$ . Acoustical measurements, relative humidity and air flow measurement were also performed but are not discussed here. Measurements are performed with none, one or two persons in the meeting room with the recirculation of the indoor unit ON or OFF. For the OFF situation the room inlet of the indoor unit was taped shut. The person(s) sat in position(s) 1 and/or 3, see figure 4. The  $\text{CO}_2$  and the particles were measured in the front and back positions at breathing zone height (1.1 m) and ceiling height (2.8 m). The persons performed standard office activities as reading and writing/typing.

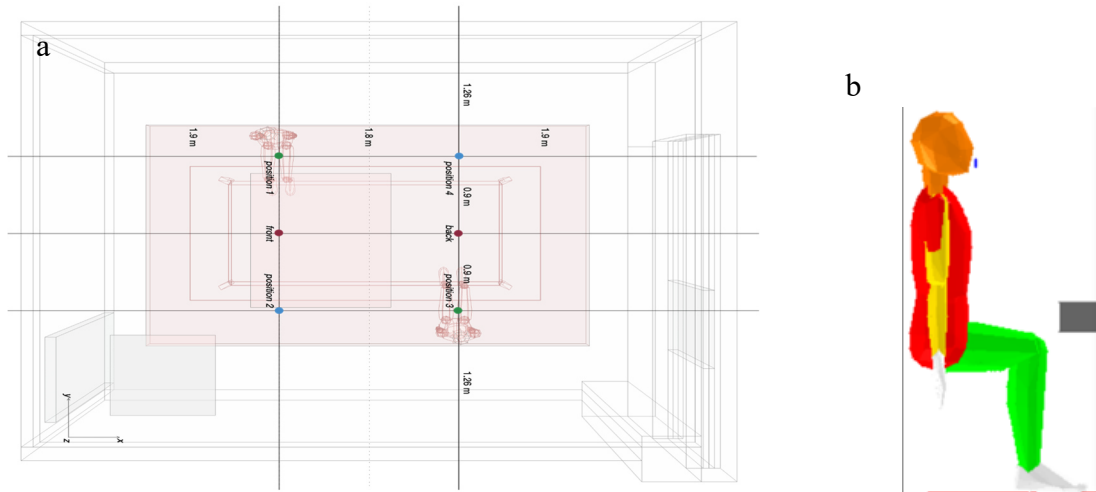


Figure 4: a. User positions and equipment locations and b. the manikin used in the simulation.

### 3.4 Simulations

The CFD-program Phoenics is used for the simulations. The simulated meeting room is also  $4.52 * 5.6 * 2.8 \text{ m}^3$ . The computational geometry replicates in detail the experiments carried out in the full-scale chamber, see Figure 4. Convergence and grid parameters can be found in Cai (2022) as the input for the indoor ventilation unit. The tracer gas is  $\text{CO}_2$  for the CFD-model calibration. The  $\text{CO}_2$ -concentration in nature is considered to be 407 ppm (at the moment already 418 ppm, see <https://www.co2.earth/daily-co2>) for the base case. In the variant simulation the outside  $\text{CO}_2$ -concentration is assumed to be 0 ppm.

The variants that are modelled are: recirculation rates of 0, 4, and 8 volumes/hour. The distance between the return and the supply is 0.0 m, 1.75 m and 2.67 m. The distance between the supply and the exhaust of 1.75 m and 2.67 m. The applied filters are M5 with 0% efficiency and F7 with 50 % efficiency). In total this leads to  $3 \times 3 \times 2 \times 2 = 36$  variants. As the  $\text{CO}_2$  is chosen as the tracer gas of choice, the resulting  $\text{CO}_2$ -concentrations with the filter in the CFD-calculations can be lower than usual (800 ppm).

### 3.5 Manikin

An adult person in rest is simulated as a manikin, see figure 4b. There are two manikins in the model. Their breathing mode is simulated by creating an inlet object at each mouth, perpendicular to the y-axis, and setting respiratory volume and  $\text{CO}_2$ -concentration rate respectively. The skin temperature of the manikins is  $34 \text{ }^\circ\text{C}$  in sitting position. The clothing insulation (Clo) is 1. The heat power of each manikin was set to 80 W. The area of oral and nasal opening is  $0.011 * 0.011 \text{ m}^2$ . The total exhaled air for each manikin in the CFD-calculation was chosen to be  $0.66 \text{ m}^3/\text{h} = 0.000183 \text{ m}^3/\text{s}$  (Villafriuela et al, 2016). The  $\text{CO}_2$ -production in the CFD-calculation was 20 l/h. This all leads to a  $\text{CO}_2$ -concentration in the exhaled air of  $20 \text{ l/h}/660 \text{ l/h} = 3.03 \%$  in the exhaled air and an exhaled air velocity of circa 1.5 m/s. In the CFD-model the exhaled air is assumed to be continuous. The sitting height is set as 1.3 m, the breathing zone for analysis is set at 1.1 m height.

## 4 RESULTS

### 4.1 Measurements

#### *Effect of position and recirculation*

As the two positions, front and back, do not have the same distance to the inlet and outlet of the indoor unit, there is a difference in CO<sub>2</sub>-concentration for the different positions, see figure 5.

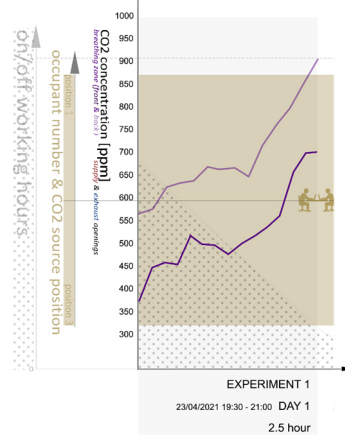


Figure 5: Scenario 1 of experiment about current situation, light line is the back position, the dark line is the front position, recirculation is ON.

The temperatures, see figure 6, show that the ventilation system is in continuous steady air supply mode when the air recirculation mode is ON with a low air exchange rate. While, when the air recirculation is OFF, the fan-coil assumes that there is a need of huge cooling load, because the temperature sensed by the system remain on a high level for a relatively long time. Thus, the ventilation is on full performance for a longer time, and in this way, the space is under a high air exchange rate. The higher air exchange rate when the air recirculation is OFF is the reason the peak value of the CO<sub>2</sub>-concentration is lower at the ceiling and the breathing zone when the air recirculation is off, see figure 7.

The particle concentration, however, shows something different, see figure 8. The particle concentration stays constant when the recirculation is OFF, and increases in the breathing zone when the recirculation is ON. This is as expected due to the higher air change rate when the recirculation is off. On the other hand, the particle concentration in the ceiling reduces when the recirculation is ON. How the air moves in the room is therefore just as important as the air change rate of fresh air. The **mixing level**, thus, is a key element in the ventilation efficiency of mixing ventilation strategy.

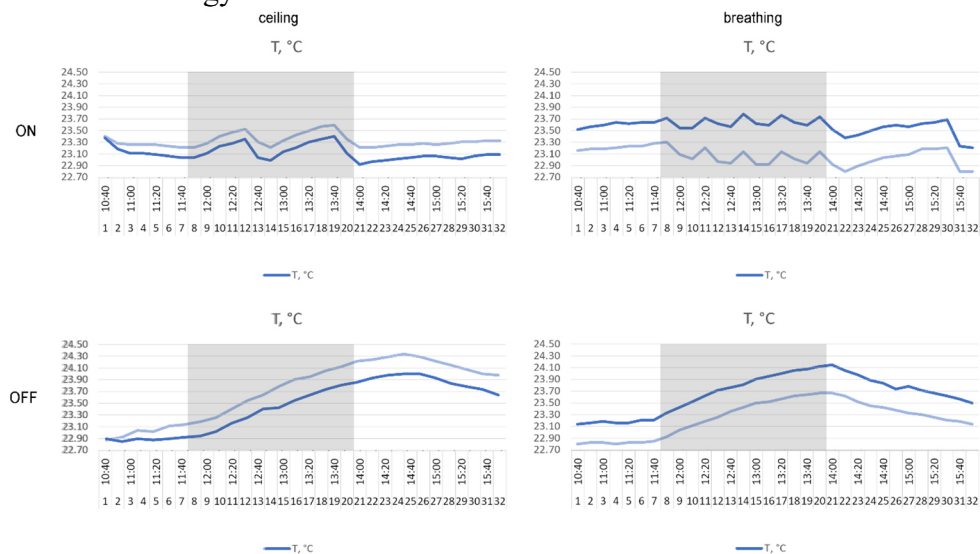


Figure 6: Temperature, light line: different position as where the particle counter is, dark line: same position as where the particle counter is.

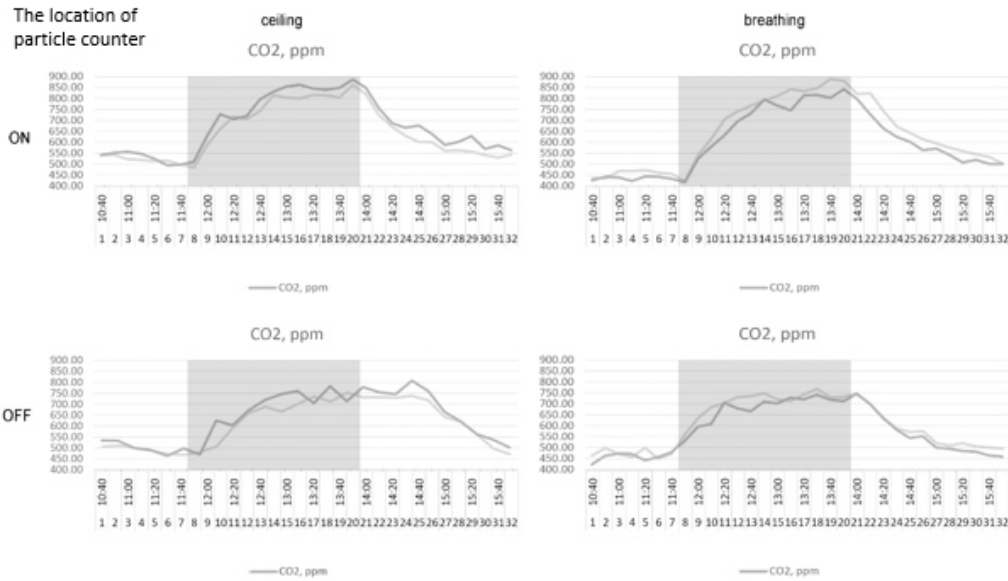


Figure 7: CO<sub>2</sub>-concentration, light line: different position as where the particle counter is, dark line, same position as where the particle counter is.

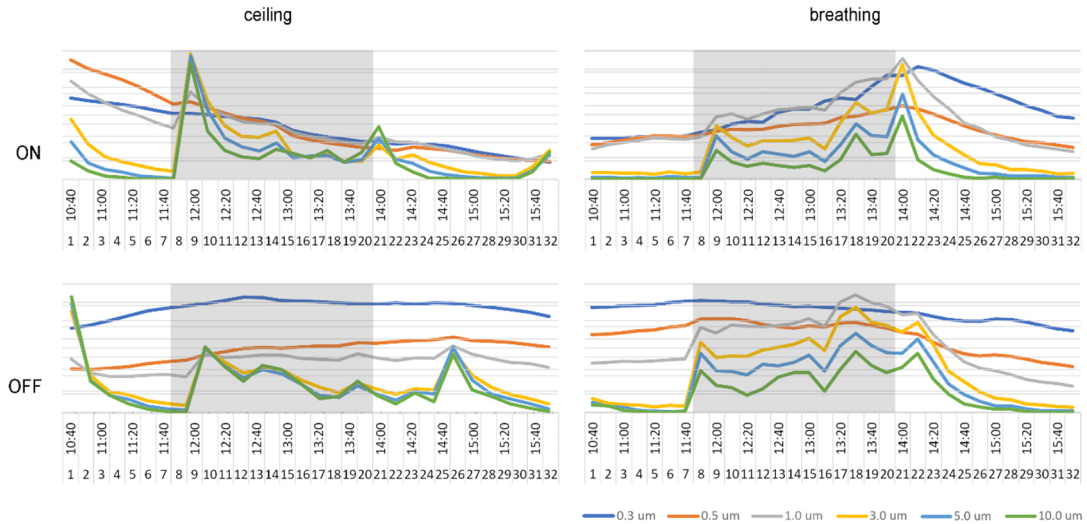


Figure 8: The measured particle concentration for different sizes of particles.

## 4.2 Results simulations

### *Infectious risk (Wells-Riley equation)*

Based on the performance of the current meeting-room the infection risk is 15% with a fresh air supply of 79 m<sup>3</sup>/h for two persons in the room with one infected person in the room for 1 hour and a infection load of 25 quanta per hour.

$$PI = \frac{c}{s} = 1 - e^{-\left(\frac{Iqpt}{Q}\right)} = 1 - e^{-\left(\frac{1 \cdot 25 \cdot 0.66}{79 \text{ m}^3} \cdot 1h\right)} = 15\%$$

When this person is for 2 hours in the meeting room the infection risk will rise to 34%.

### *CFD-modelling*

The CFD-modelling simulated the Covid-19 virus by using CO<sub>2</sub> as a tracer gas. In figure 9 the CO<sub>2</sub>-concentration in the breathing zone under this type of ventilation is 915 ppm for the standard case, which is consistent with the on-site measurement results.

The CFD model of the standard case has an air change efficiency,  $\epsilon^a$ , of 51%, which is very close to the 50% of a well-mixed ventilation pattern, see table 1.

The local air change efficiency in the breathing zones is  $> 100\%$ , which means the air change in the breathing zones is above the average air change efficiency of the whole space. The general pollutant removal efficiency is  $82\%$  for the whole space. The local pollutant removal efficiency is  $102\%$  in the breathing zones which means that the air quality in the breathing zone is good and better than the general air quality in the room.

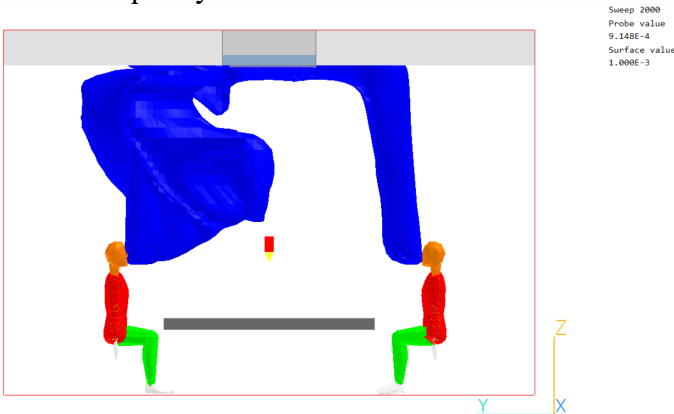


Figure 9: The outcome of the simulation of the current ventilation environment

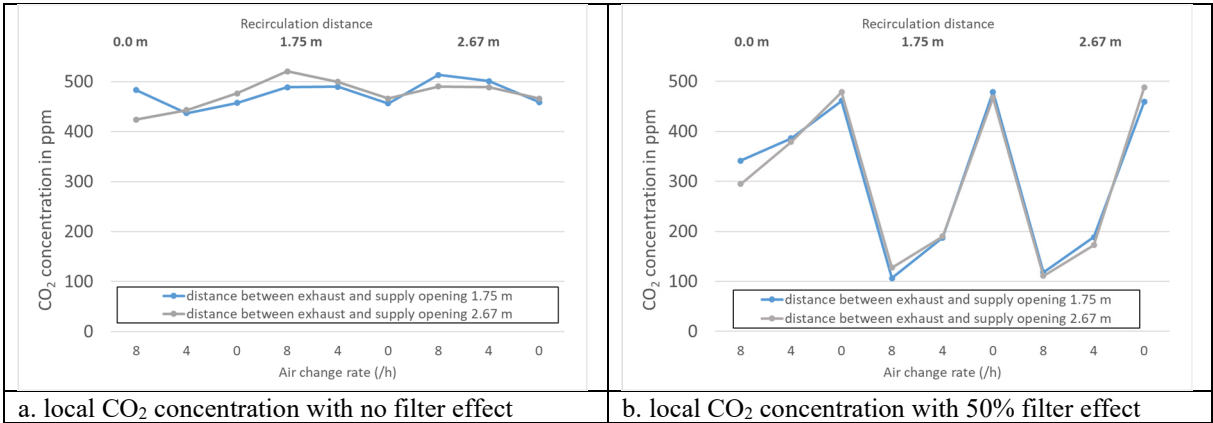
Table 1: Simulated standard case

		General	Local Position 1	Local Position 2
Ventilation efficiency	Air change efficiency	51%	$>100\%$	$>100\%$
	Pollutant removal efficiency	82%	102%	102%

**Simulation of the variants**

The cases where a 50% filter was applied differ significantly from the cases without a filter, see **Error! Reference source not found.** a and b. The 50% filter causes the local CO<sub>2</sub> concentration to generally drop to 20% of the cases without a filter. Only the cases without air recirculation where the application of a filter is necessary and efficient in most cases, except the cases without air recirculation. The CO<sub>2</sub>-concentration outside is not taken into account and the filter is assumed to filter out the CO<sub>2</sub>-particles as proxy for the virus particles.

The gaps (see figure 9) between red and blue lines illustrate the impacts from general ventilation distance, between supply and exhaust openings. In both cases, when there is 50% filter effect or no filter effect in the ventilation system, larger general ventilation distances help decreasing the local CO<sub>2</sub>-concentration, but the differences are small, a maximum around 50 ppm. Thus, enlarging the general ventilation is a less effective way to enhance the “corona-proof” performance of the ventilation system in the medium-scale environment, compared with enlarging the distance between the supply and return opening.



a. local CO<sub>2</sub> concentration with no filter effect

b. local CO<sub>2</sub> concentration with 50% filter effect

Figure10: CO<sub>2</sub> concentrations in the breathing zone. The outside CO<sub>2</sub>-concentration is assumed to be 0 ppm.



## 5 DESIGN IDEA

Based on the results from the simulations, a recirculation system with a large distance between the exhaust and the supply opening gives the best results. The new design has 4 return openings with a large distance between the return and the supply openings, see figure 11. Normally the supply openings are at the underside of the fan-coil near the ceiling and the return openings are in between both supply openings as shown in figure 3, which produces short-circuiting of air flows.



Figure 11: 2The draft ventilation renovation product model

### 5.1 Test of the Design

The new ventilation unit design is tested by CFD simulations, see Cai (2022), and measurements of CO<sub>2</sub> and particles of 0.3 μm. The ventilation unit with the extended recirculation positions and the filter is compared with the ventilation unit without recirculation. The temperatures between the two different experiments were between 21.7 and 22.3 °C for both experiments and can be assumed to be constant. The air change rates of the room for both measurements is almost the same suggesting that the experiments are based on the same ventilation mode. The CO<sub>2</sub>-concentrations of the two experiments were within 50 ppm difference also supporting the assumption of a similar ventilation working mode, see figure 12. After the users entered the room, the CO<sub>2</sub>-concentration for the new design case is always lower than in original case without recirculation. Since the filter cannot remove CO<sub>2</sub>, particles, measurements were applied to see the impact of the design synergised with the rough filter. When the filter is applied for airborne particles (0.3 μm), the smart building system and indoor facilities started fully working on first day in the morning and until 11:20 am they are at the same start value for both days for both the CO<sub>2</sub> and particle measurements. As long as the system works, the indoor particle count will drop until around 75,000.

The local particle concentration in the new-design case is always lower than that in the case without recirculation case. The peak value difference can achieve 1/3rd of the particle concentration in the case without recirculation when users left the room.

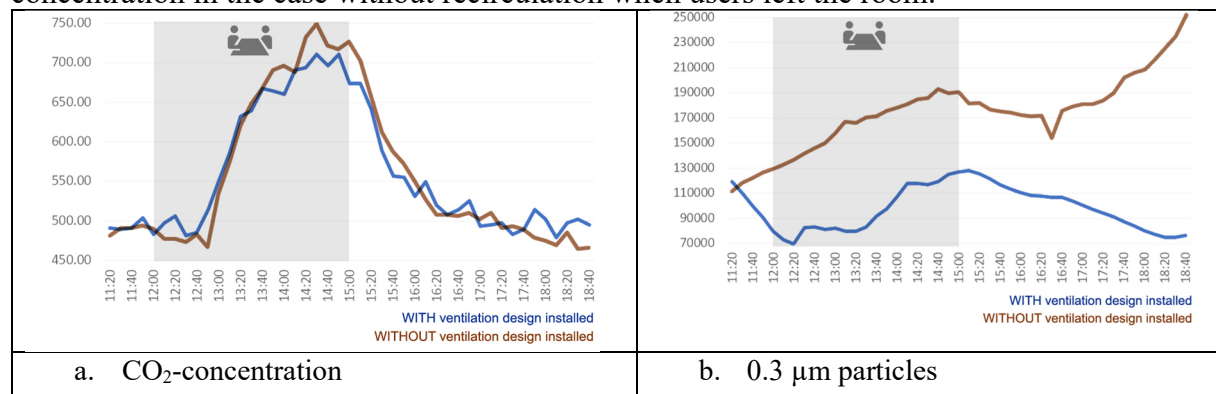


Figure 12: CO<sub>2</sub> and 0.3 μm particle number changes WITH/WITHOUT ventilation design installed, shadow duration is when two users were indoors

## 6 CONCLUSIONS

A new ventilation design using recirculation, a larger distance between supply and extract for recirculation and a 50 % filter reduces the amount of 0.3  $\mu\text{m}$  particles to 33% with the same outside air change rate. A 5% indoor infection risk rate referring to the contaminant concentration decreasing rate in CFD analysis can be obtained in this way.

Based on CFD-simulations an infection risk below 1 % should be possible, for instance with a low-pressure filter with an efficiency around 99 %. This could be realized with an electrostatic precipitator (filter), see [Virus Free \(virus-free.nl\)](https://virus-free.nl/).

## 7 ACKNOWLEDGEMENTS

Kuijpers is a company with years of experience in technical installations in buildings whose service includes design, construction and maintenance. The company pays special attentions to a healthy working and living environment. As the clean room contractor for Johnson & Johnson's Dutch vaccine plant, Kuijpers actively responds to the Dutch epidemic prevention request and explored COVID-19 related epidemic prevention research.

## 8 REFERENCES

Cai Wenyan (2022) Graduation Thesis, <http://resolver.tudelft.nl/uuid:674a3a82-d738-42d2-8f8e-50c5992cba1e>

Dai, H., & Zhao, B. (2020). *Association of the infection probability of COVID-19 with ventilation rates in confined spaces*. Building Simulation, 13(6), 1321–1327 [doi.org/10.1007/s12273-020-0703-5](https://doi.org/10.1007/s12273-020-0703-5)

Ding, Er; Zhang, Dadi; Bluysen, Philomena M. (2022) *Ventilation regimes of school classrooms against airborne transmission of infectious respiratory droplets, A review*, Building and Environment, Volume 207, Part A, [doi.org/10.1016/j.buildenv.2021.108484](https://doi.org/10.1016/j.buildenv.2021.108484)

Lipinski, T., Ahmad, D., Serey, N., & Jouhara, H. (2020). *Review of ventilation strategies to reduce the risk of disease transmission in high occupancy buildings*. International Journal of Thermofluids, 7–8, 100045. <https://doi.org/10.1016/j.ijft.2020.100045>

Mateescu, C. (2018). *What is the CO<sub>2</sub> generation (ppm/h) by a human at different levels of exercises?*

Morawska L., G.R. Johnson, Z.D. Ristovski, M. Hargreaves, K. Mengersen, S. Corbett, C.Y.H. Chao, Y. Li, D. Katoshevski (2009) *Size distribution and sites of origin of droplets expelled from the human respiratory tract during expiratory activities*, Aerosol Science 40, 256-269, [doi:10.1016/j.jaerosci.2008.11.002](https://doi.org/10.1016/j.jaerosci.2008.11.002)

Morawska, L et al. (2020). *How can airborne transmission of COVID-19 indoors be minimised?* Environment International, 142. <https://doi.org/10.1016/j.envint.2020.10583>

Mundt M., H. M. Mathisen, M. Moser, P. V. Nielsen. (2004). *Ventilation Effectiveness: Rehva Guidebook*; Federation of European Heating and Ventilation Association, ISBN-10 2960046803

Nafezarefi, F; Joosten, P. (2020). *Oplossingen voor zuivere lucht in gesloten ruimtes*. TVVL Magazine, 05, 36–42.

Randall K, Ewing ET, Marr LC, Jimenez JL, Bourouiba L. (2021) *How did we get here: what are droplets and aerosols and how far do they go? A historical perspective on the transmission of respiratory infectious diseases*. Interface Focus, vol. 11, 6, <https://doi.org/10.1098/rsfs.2021.0049>

Sze To, G. N., & Chao, C. Y. H. (2010). *Review and comparison between the Wells-Riley and dose-response approaches to risk assessment of infectious respiratory diseases*. Indoor Air, 20(1), 2–16. <https://doi.org/10.1111/j.1600-0668.2009.00621.x>

Villafruela JM, Olmedo I, San José. *Influence of human breathing modes on airborne cross infection risk*. Building and Environment 106 (2016) 340-351.

- *COVID-19 death rate by country* | Statista. (2021). Retrieved 6 January 2021 and 24 November 2021, from <https://www.statista.com/statistics/1105914/coronavirus-death-rates-worldwide>
- Virus Free: <https://virus-free.nl/>
- [www.co2.earth/daily-co2](https://www.co2.earth/daily-co2)
- [www.nuffieldtrust.org.uk/resource/cancer-survival-rates#background](https://www.nuffieldtrust.org.uk/resource/cancer-survival-rates#background)